Automated Liver Disease Detection Through Lesion Skin Analysis Using 7 Convolutional Neural Network (CNN) Machine Learning Algorithms

Jessica S. Velasco[1], Karla A. Dela Cruz[1], Jan-Jemil A. Datay[1], Jen Kylee d. Mendoza[1], Aivan Allen N. Siquig[1], Jayson R. Tindugan[1]

[1]jessica.velasco@tup.edu.ph,
[2]karla.delacruz@tup.edu.ph,
[3]janjemil.datay@tup.edu.ph,
[4]jenkylee.mendoza@tup.edu.ph,
[5]aivanallen.siquig@tup.edu.ph,
[6]jayson.tindugan@tup.edu.ph

[1]Department of Electronics Engineering, College of Engineering, Technological University of the Philippines, Manila, Philippines

Abstract— **The liver organ plays a vital role in the body, and early detection of liver diseases can be lifesaving. Despite the rapid increase in the number of individuals with liver diseases in recent years, identifying the symptoms of such diseases remains a challenge. Skin diseases often have underlying organ-related disorders, and liver disease is one of the most common conditions associa ted with skin manifestations. In this study, the researchers integrated an Analytic Camera and developed a mobile application (Liverify App) for automated liver disease detection using lesion skin analysis. The study assessed the accuracy in detecting liver diseases and liver stage/s through the 5 skin manifestations (Spider Angioma, Purpura, Eruptive Xanthoma, Xanthelasma, and Leukocytoclastic Vasculitis) using 7 Convolutional Neural Network models (YOLO v5, DenseNet, MobileNet, VGG 16, Xception, ResNet-50, and Inception-Resnet v2). The researchers trained and tested the different Machine learning algorithms with 7,922 datasets. Validation tests were conducted to identify the CNN model with the highest accuracy for liver disease detection through lesion skin analysis. Based on 210 tests, YOLO v5 was found to be the most effective CNN model using the Analytic Camera with 100% accuracy, while the mobile application (Liverify App) has 73.33% accuracy. The functionality of the device and application were evaluated based on the validation tests, a clinical test (liver patient), and by a resident Gastroenterologist at Justice Jose Abad Santos General Hospital, Internal Medicine Department. Overall, the Analytic Camera as a computer-aided diagnostic device can help improve the accuracy and efficiency of liver disease diagnoses and treatments. It can serve as an alternative to the conventional and costly laboratory tests in regions lacking a specialized liver expert or in hospitals that do not have an Internal Medicine Department.**

Keywords— Liver disease, Liver disease detection, Lesion Skin Analysis, Central Neural Network (CNN) Models

I. INTRODUCTION

Skin diseases are conditions that affect the skin. This may cause rashes, inflammation, itchiness, and/or other skin changes [1]. Most skin lesions have underlying disorders or internal organ-related diseases which can range from the very subtle to the more obvious.

The most prevalent skin manifestation related to organs is the liver. This is one of the extrahepatic signs of liver disease which can aid in the early diagnosis and treatment of liver diseases [2]. Liver disease is a general term that covers all the potential problems that cause the liver to fail to perform its designated functions. It is also referred to as a hepatic disease. Usually, more than 75% or three-quarters of liver tissue needs to be affected before a decrease in function occurs [3]. Liver disease has many causes. It is either through infection, immune system abnormality, genetics, cancers, or might chronic alcohol abuse, fat accumulation in the liver, certain prescription or over-the-counter medications, certain herbal compounds, etc. Over time, conditions that damage the liver can lead to scarring (cirrhosis), which can lead to liver failure, a life-threatening condition if not yet diagnosed and treated early on [4].

In 2020, the number of deaths in the Philippines related to liver diseases reached 7,076. The country ranks 135th in liver disease-related deaths with a death rate of 8.65 per 100,000 of the population. Liver cancer and liver diseases rank 18th and 19th respectively in the leading causes of death in the Philippines [5]. However, according to the report in 2021 by the World Health Organization, Hepatitis B is a viral and potentially life-threatening liver infection that attacks the liver and can cause both acute and chronic disease. It estimates that 296 million people were living with chronic hepatitis B infection in 2019, with 1.5 million new infections each year. In 2019, hepatitis B resulted in an estimated 820 000 deaths, mostly from cirrhosis and hepatocellular carcinoma (primary liver cancer) [6].

Some of the skin manifestations of liver disease are Spider Angioma, Purpura, Eruptive Xanthoma, Xanthelasma, and Leukocytoclastic Vasculitis. These conditions are related to Chronic Liver Disease, Chronic Hepatic diseases, Hepatic Stigmata, Hepatitis, etc. [7].

However, these skin manifestations showed that the damage in the liver is approximately 75% because the symptoms are already visible outside the body. Therefore, there are six stages of liver progression that can determine the stage of the liver based on the symptoms that occurred. These are the healthy liver, hepatitis (inflammation), fibrosis (scarring), cirrhosis (severe scarring), liver cancer, and liver failure [8].

The advancement of technology today helps to understand the lesion skin and analyze the different dermatological conditions through microscopy and other laboratory tests as the traditional way of identification is being practiced. However, Machine Learning of automatic analysis and image segmentation can help better easily link these skin symptoms to the different diseases externally and internally upon studying.

II. RELATED STUDIES

Skin symptoms are frequently an indication of underlying systemic disease. The liver is one of the most common organs in the body; the skin manifestations of liver diseases are very visible. It's essential to remember, however, that these cutaneous signs can indicate underlying liver disease and frequently appear in the context of hepatic dysfunction [13].

Spider angioma is a benign vascular lesion that looks like a spider's body and is characterized by unusual end vascular dilation. The lesion has a center area and extensions that extend outward like the body of a spider. Spider angiomas can show as a single or numerous lesions on the skin surface of the face, neck, chest, and arms; these lesions have only been seen in the sublingual mucosa and the stomach on rare occasions, and they have never been seen in the nasal mucosa [14].

The upper trunk is the most common site for spider angiomas. Blanching is caused by compression of the lesion. Spider angiomas aren't always associated with cirrhosis; they can also appear in patients taking oral estrogens or who are pregnant. The existence of spider angiomas has been linked to elevated estrogen levels. According to one study, spider angiomas were seen in 50% of alcoholic cirrhotic patients compared to 27% of nonalcoholic cirrhotic patients. Spider angiomas were seen in 33% of patients with cirrhosis [15]. A severe case of jaundice in a patient with a long history of alcohol abuse led to a questionable diagnosis of liver cirrhosis. A physical examination found a man suffering from moderate acute pain, considerable jaundice, and a diffusely uncomfortable tummy on the touch. There were two spider angiomas, caput medusae, and mild asterixis on the torso [16].

Eruptive xanthomas are skin manifestations associated with hypertriglyceridemia. As a result, lowering hypertriglyceridemia can help to alleviate this disease. Eruptive xanthomas may signal metabolic issues linked to atherosclerosis. Eruptive xanthoma can assist doctors to diagnose hypertriglyceridemia and insulin insensitivity caused by obesity and diabetes, as well as hereditary abnormalities affecting lipoprotein metabolism. Skin symptoms of metabolic diseases, which might contribute to atherosclerosis, should be recognized by clinicians [17].

Localized lipid deposits in the skin or subcutaneous tissue are known as eruptive xanthomas and are linked to both primary and secondary hyperlipidemia. Small yellow papules on the buttocks or extensor surfaces are a common symptom. Eruptive xanthomas may not be extremely rare, they are often underdiagnosed. Eruptive xanthomas are strongly associated with primary and secondary causes of hyperlipidemia. The potential consequences of hypertriglyceridemia can be severe, as the risk of cardiovascular disease and pancreatitis increase exponentially [18].

Eruptive xanthoma should be recognized as an indicator of underlying systemic conditions such as hypertriglyceridemia and uncontrolled diabetes mellitus to prevent pancreatitis and cardiovascular disease. Professionals must notice it to avoid subsequent consequences such as pancreatitis and cardiovascular disease [19].

Eruptive xanthoma is distinguished by an acute, widespread papular rash that often affects the back, buttocks, and extremities. Hyperlipidemia, hypertriglyceridemia, and an elevated long-term risk of atherosclerotic cardiovascular disease are all related to eruptive xanthoma. There are currently no professional guidelines specific to the medical treatment of cutaneous xanthomas. The treatment of eruptive xanthomas is dependent upon correcting underlying blood lipid imbalances through lifestyle modification and pharmacological therapy [20].

Asymptomatic skin lesions to acute itch and discomfort are common clinical manifestations. The appearance of eruptive xanthomas might indicate the beginning of significant problems. Prompt detection of such skin manifestations is required to prevent the development of potentially lethal medical conditions such as coronary artery disease and pancreatitis [21].

The most frequent cutaneous xanthoma is Xanthelasma Palpebrarum (XP), which is characterized by sharply delineated yellowish flat plaques on the upper and lower eyelids, primarily towards the inner canthus bilaterally. Although the specific origin is unknown, lipid imbalances, hormonal variables, local factors, and macrophages are thought to have a part in its etiopathogenesis. XP can be caused by lipid metabolic problems or essential familial hypercholesterolemia, in which high levels of low-density lipoprotein (LDL) are identified due to a malfunction in the LDL receptor, which causes improper uptake and breakdown, resulting in skin lesions [22].

Xanthelasma Palpebrarum is a benign disorder with few significant implications, however, it does impact the patient's physical appearance. Among patients with fatty liver, individuals presenting with XP showed higher serum levels of total cholesterol, fasting glucose, and low-density lipoprotein than those without XP. Individuals with non-alcoholic steatohepatitis had higher Z scores of xanthelasma in gene expression analyses than those without non-alcoholic steatohepatitis. The findings imply that those with XP are more likely to develop Non-Alcoholic Fatty Liver Disease (NAFLD) and have more severe dyslipidemia [23].

The most frequent cutaneous xanthoma discovered on the medial side of the eyelid is Xanthelasma palpebrarum. A typical lesion is a flat, yellowish plaque on the skin. However, we report on a rare incidence of intramuscular xanthoma discovered during blepharoplasty

for ptosis correction. A 53-year-old male patient presented to our clinic complaining of a ptotic eyelid. He was concerned about his physical look and the discomfort he felt while opening his eyes, and he wanted both issues resolved. During the procedure, a yellowish plaque around 0.30.3 cm in size was discovered in the orbicularis oculi muscle. The lesion was removed, and biopsies revealed xanthelasma. This particular example of xanthelasma palpebrarum was discovered in a single muscle. As a result, individuals with these lesions require a cautious approach to clinical and histologic assessment and imaging [24].

Leukocytoclastic vasculitis is a rare extrahepatic symptom of hepatitis C virus infection (HCV). The case of a patient was presented who received a liver transplant to treat cirrhosis and hepatocellular carcinoma caused by HCV infection, but experienced skin lesions and systemic symptoms like fever after the procedure. The patient demonstrated total remission of all symptoms shortly after starting HCV antiviral medication. While there have been earlier reports of leukocytoclastic vasculitis in solid organ transplant patients, no previous case of this being a sign of HCV recurrence in this context has been reported in the literature. The challenge of correctly diagnosing HCV-associated leukocytoclastic vasculitis after liver transplantation lies in the many immunological and infectious agents that can cause similar skin lesions in immunosuppressed patients [25].

Most of these responses are seen with the messenger ribonucleic acid-based Pfizer/BioNTech (BNT162b2) and Moderna (mRNA-1273) COVID-19 vaccines. They present two cases of leukocytoclastic vasculitis following ChAdOx1 nCoV-19 coronavirus vaccination (recombinant), highlighting potential novel dermatological symptoms of the recombinant coronavirus vaccine being used in Europe, South America, and Asia [26].

Vaccines can cause cutaneous adverse effects owing to nonspecific inflammation or immune-mediated reactions. Several kinds of vasculitis have been observed. The case of a 71-year-old lady who developed cutaneous small-vessel vasculitis following the second dose of Vaxzevria COVID-19 immunization, with histological evaluation of a skin sample revealing leukocytoclastic vasculitis. Cutaneous small-vessel vasculitis is an uncommon illness that can be idiopathic or related to underlying infections, connective tissue abnormalities, cancer, or medicines. Immune complex deposition in tiny blood arteries causes complement activation and leukocyte recruitment. Exacerbation of small-vessel vasculitis has been documented following the administration of many vaccinations, notably the influenza vaccine [27].

Purpura has been linked to a variety of infectious origins, some of which are potentially fatal. Purpura is caused by trauma to the skin's blood vessels, resulting in hemorrhage into the surrounding tissue. Pressure does not blanch lesions. Direct trauma, endothelial infection (e.g., rickettsial infection, meningococcemia), vessel occlusion, immune complex deposition, platelet depletion or dysfunction, or other conditions that cause erythrocyte leakage into the skin, mucous membranes, conjunctivae, or retina can all cause vessel damage [28].

Liver diseases have different stages: Healthy Liver, Hepatitis (Inflammation), Fibrosis (Scarring), Cirrhosis (Severe Scarring), Liver Cancer, and Liver Transplantation [9]. Infections, hereditary disorders, obesity, and alcohol abuse are among the factors that can lead to liver disease. Liver illness can cause scarring and more serious problems over time. Early treatment can assist in the healing of the damage and the prevention of liver failure [1].

Hepatitis is a liver infection that causes inflammation. The most prevalent skin symptoms in hepatitis C patients were pruritus, LP, and cryoglobulinemia. The cutaneous symptoms of HCV infection place a significant cost on public health and have negative consequences for patients. This study emphasizes the importance of HCV screening in patients with diverse cutaneous illnesses to give early diagnosis and treatment for HCV infection and prevent the disease from spreading further. Understanding the dermatological disorders linked with hepatitis C is crucial because it can aid in early identification and treatment [29].

Other than the liver, the Hepatitis C virus (HCV) has been demonstrated to infect a variety of tissues. However, only a handful of the various extrahepatic manifestations (EMs) of HCV, such as cryoglobulinemia, lymphoma, insulin resistance, type 2 diabetes, and neurological diseases, have been proven to be directly connected to HCV infection of extrahepatic tissues. The majority of EMs are caused by HCV-triggered immune-mediated mechanisms. It is anticipated that up to 74% of chronic hepatitis C patients would acquire at least one EM. Although not all HCV patients with EMs may resolve with the sustained virological response, all should be investigated for antiviral treatment [30].

A variety of rheumatologic symptoms can confound the diagnostic approach and modify the natural history of primary liver disease, often worsening prognosis due to concomitant multiple organ failure. These symptoms can occur in conjunction with a variety of liver illnesses, including viral hepatitis, autoimmune hepatitis, alcoholic liver disease, nonalcoholic fatty liver disease, hemochromatosis, and Wilson's disease. Not only rheumatologists but also other doctors must be aware that these unusual signs may indicate an undetected liver illness [31].

In the study of 100 patients having a chronic liver disease (CLD), the skin, mucosal, nail, and hair manifestations, Pruritus was the most prevalent (25 percent) and Dupuytren contracture was the least common (3 percent). In terms of mucosal manifestations, oral lichen planus (LP) was the most common (34 percent), leukonychia was the most common (21 percent), and hair sparse axillary and pubic hair was the most common (50 percent). According to the findings, there seems to be a variety of skin, mouth, hair, and nail manifestations that vary depending on the stage of the disease [14].

Cirrhosis is caused by viral hepatitis. Hepatitis is caused by two viruses: hepatitis B and C. Excessive consumption of alcoholic beverages, as well as other variables that can affect the liver, can cause it. A software application based on the certainty factor (CF) technique is used to detect cirrhosis. Each symptom was given with certainty by a doctor, and the cirrhosis results and indicators were also verified by an expert. This expert system was discovered to help support users in the early diagnosis of cirrhosis. The expert system is effective at

detecting cirrhosis based on the illness symptoms chosen by the user [32].

Skin symptoms of systemic illnesses assist in identifying the organ affected and the likely disease-causing damage. Skin changes associated with liver cirrhosis are not specific, as they can be found in illnesses other than those involving the liver. Thus, a combination of skin alterations and systemic symptoms may aid in identifying the disease-causing liver cirrhosis. Pruritus is one of the most prevalent and distressing signs of liver cirrhosis, negatively impacting the quality of life and necessitating additional research into cirrhosis cutaneous manifestations. Spider telangiectasia, palmar erythema, paper money skin, xanthomas, pigmentation changes, nutritional deficits, hair changes, and nail alterations are examples of nonspecific cutaneous symptoms [2].

The potential of neural network models to predict the possibility of liver failure in an ICU patient many hours before conventional screening protocols have been proven. External validation of this model's performance was done using data from critical care patients from a separate database, and it attained a high sensitivity of 83.3 percent and a specificity of 77.5 percent. Furthermore, at a median of 17.5 hours before the start of liver failure, this model identified 83.5 percent (N=525) of liver failure patients. The model-generated LFRI's predicted accuracy is improved. Model performance will be improved in the future by examining various sets of model inputs and predictors, as previously indicated. The construction of patient population-specific models for future inclusions. These models are rising in popularity among research groups across the world due to their ability to improve clinical treatment by predicting therapy outcomes, enhancing diagnosis, and informing the design of surgical platforms and patient development [33]. Skin diseases are one of the most widely prevalent diseases in the world. Because of the challenges in skin texture, hair presence, and color, diagnosing them is quite tough. To improve the accuracy of diagnosis for various types of skin diseases, approaches such as machine learning must be developed. In the medical field, machine learning techniques are commonly employed for diagnosis. These algorithms make decisions based on feature values from photos. The feature extraction stage, the training stage, and the testing stage are the three stages of the procedure. Machine learning technology is used to train the procedure with different skin pictures [34].

Over the last two decades, computer-aided detection or diagnosis (CAD) has been a promising field of study. Medical image analysis seeks to make radiologists' and doctors' diagnostic and treatment processes more efficient [35]. To enhance exam precision, enhance consistency in image interpretation, assist prognosis assessment, and assist treatment decision-making, computer-aided diagnostic (CAD) systems have been developed [36].

The 2019 study demonstrates that CNN-based approaches in CAD research will considerably aid the advancement of medical image analysis, and the future directions may be toward radiomics, precision medicine, and imaging grouping. Additionally, the distinctive features of transfer learning may accelerate the development of CAD systems for diverse diseases and imaging modalities [35]. In the 2018 research, the effectiveness of these CADs is based on the features that are extracted (using statistical, structural, and spectral approaches), as well as the type of classifier (neural network, SVM, Bayesian, KNN, minimum distance, and regression). It is preferable to act based on statistical descriptors of intensity histograms as well as methods that include information on the location of pixels relative to each other to extract the useful features of images from the existing set of properties. Finally, the kind of classifier may have an impact on how accurately the final diagnosis is made [37].

Medical professionals are very concerned about dermatological disorders. The number of people who suffer from skin illnesses is increasing at an alarming rate as a result of rising pollution and inadequate nutrition. People frequently ignore the early indications of skin diseases. Currently, doctors evaluate and conduct a biopsy procedure to diagnose and treat skin disorders. With optimization methods, human judgment may be eliminated, producing optimistic results quickly. A thorough examination suggests that frameworks for recognizing various skin disorders may be built using deep learning techniques [38].

The recent studies effectively proposed (CNN-SVM-MAA) system which combines a Convolutional Neural Network with a Support Vector Machine classifier to develop a Mobile Android Application. Like, for the 2021 study that demonstrates the modified pre-trained model of Convolutional neural network and SVM Algorithm for the mobile application the trained and test dataset consists of around 3000 images collected from a lot of sources like Beni-Suef University Hospital, Cairo University Hospital, and various websites which are dedicated towards skin diseases and its cure to be more accurate and realistic [39]. In the 2019 study, a total of 3,406 images were studied using various sampling methods and preparation of input data, and it is considered an unbalanced dataset due to the unequal quantity of images in its classes. The accuracy was 84.28 % while using an under-sampling strategy and the default preprocessing of input data. Using an unbalanced dataset and the default preprocessing of input data, the accuracy was 93.6 %. The researchers next experimented with oversampling the dataset, and the model achieved 91.8 %. Lastly, the oversampling approach and data augmentation on preprocessing the input data produce 94.4 %, and this model was implemented on the built Android application [40]. Furthermore, N. S. Alkolifi Alenezi conducted research that used pre-trained convolutional neural networks (AlexNet) and SVM as detection methods. The database has 80 images of each illness (20 normal images, 20 melanoma images, 20 eczema images, and 20 psoriasis images) gathered from different skin disease websites. The approach works on the inputs of a color image. The image is then resized to extract features using a pre-trained convolutional neural network. After that, the feature was categorized using Multiclass SVM, and the results were displayed to the user, including the kind of disease, spread, and severity. The technology correctly diagnoses three distinct forms of skin disorders with a 100% accuracy rate [41].

III. METHODOLOGY

The research design for this study is developmental research. A systematic study of designing an analytic

camera and developing an application that can display the result findings of the processed image through Machine Learning Algorithms to identify the lesion skin to diagnose the liver disease/s associated with it and determine the liver stage.

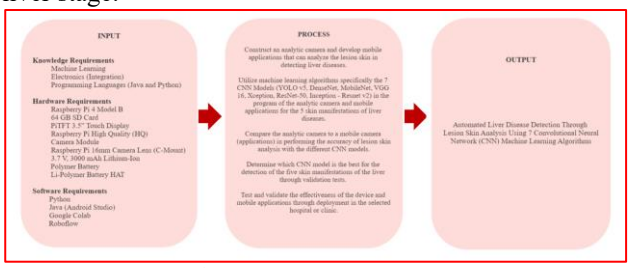

Fig. 1. Input-Process-Output

This Input-Process-Output (IPO) will serve as a guide for researchers to start and complete the necessary processes to achieve the desired outcome of the study.

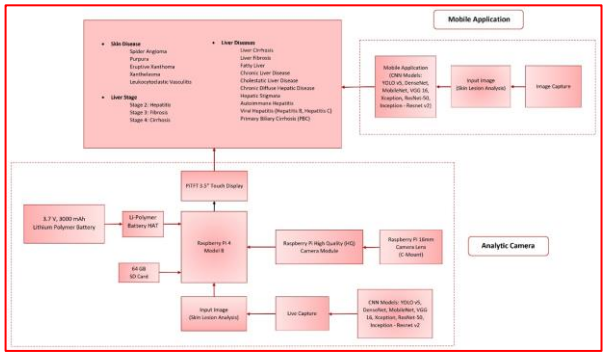

Fig. 2. Block Diagram

The Fig. 2 shows the overall block diagram of the study. This will be a guide for the processes of hardware and software developments.

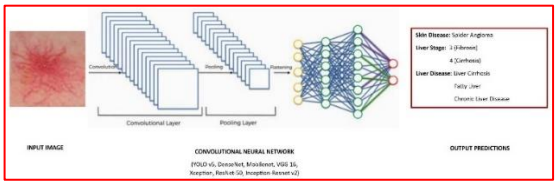

Fig. 3. Spider Angioma Convolutional Neural Network Process

The Fig. 3 shows the detection and analyzation processes of the Spider Angioma in the device and mobile application using different machine learning algorithms of the study. The liver stages (3 – Fibrosis, 4-Cirrhosis) and liver diseases (Liver Cirrhosis, Fatty Liver, Chronic Liver Disease) shown are in the range which means that the output predictions do not accurately have all of it. Still, the final diagnosis will be by a liver specialist (Hepatologist).

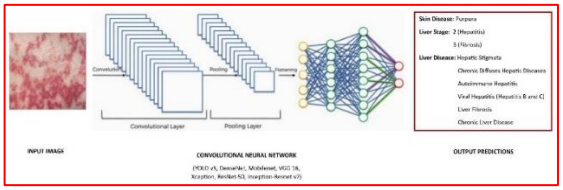

Fig. 4. Purpura Convolutional Neural Network Process

The Fig 4 shows the detection and analyzation processes of the Purpura in the device and mobile application using different machine learning algorithms of the study. The liver stages (2 – Hepatitis, 3 – Fibrosis) and liver diseases (Hepatic Stigmata, Chronic Diffuses Hepatic Diseases, Autoimmune Hepatitis, Viral Hepatitis, Liver Fibrosis, Chronic Liver Diseases) shown are in the range which means that the output predictions do not accurately have all of it. Still, the final diagnosis will be by a liver specialist (Hepatologist).

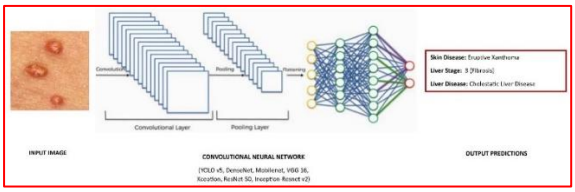

Fig. 5. Eruptive Xanthoma Convolutional Neural Network Process

The Fig. 5 shows the detection and analyzation processes of the Eruptive Xanthoma in the device and mobile application using different machine learning algorithms of the study. The liver stage (3 – Fibrosis) and liver disease (Cholestatic Liver Disease) shown are in the range which means that the output predictions do not accurately have all of it. Still, the final diagnosis will be by a liver specialist (Hepatologist).

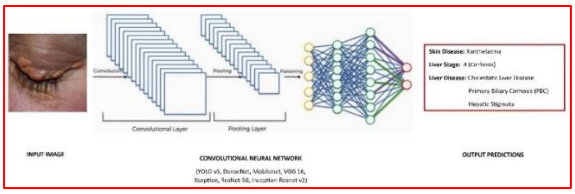

Fig. 6. Xanthelasma Convolutional Neural Network Process

The Fig. 6 shows the detection and analyzation processes of the Xanthelasma in the device and mobile application using different machine learning algorithms of the study. The liver stage (4-Cirrhosis) and liver diseases (Cholestatic Liver Disease, Primary Biliary Cirrhosis, Hepatic Stigmata) shown are in the range which means that the output predictions do not accurately have all of it. Still, the final diagnosis will be by a liver specialist (Hepatologist).

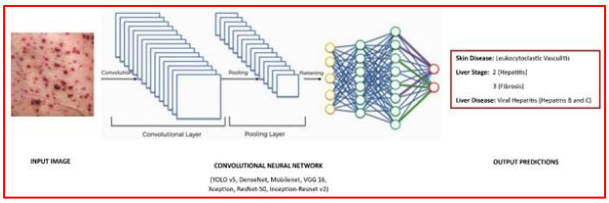

Fig. 7. Leukocytoclastic Vasculitis Convolutional Neural Network Process

The Fig. 7 shows the detection and analyzation processes of the Spider Angioma in the device and mobile application using different machine learning algorithms of the study. The liver stages (2 – Hepatitis, 3 – Fibrosis) and liver disease (Viral Hepatitis) shown are in the range which means that the output predictions do not accurately have all of it. Still, the final diagnosis will be by a liver specialist (Hepatologist).

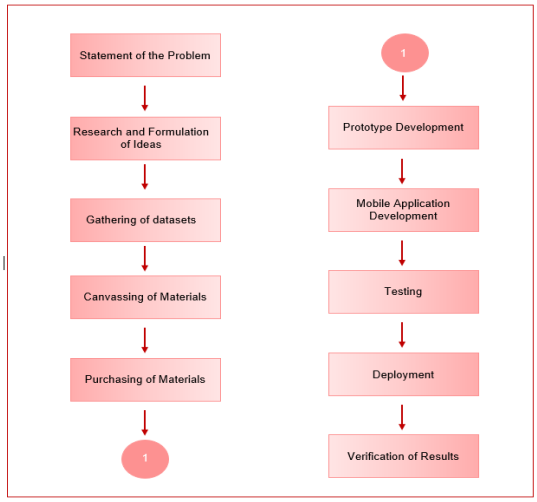

Fig.8. Research Process Flow

This Fig. 8 will serve as a guide for researchers as they follow the study's progress and complete the necessary processes to reach the final stage of verification. This arrangement will aid in meeting the study's objectives and completing the research.

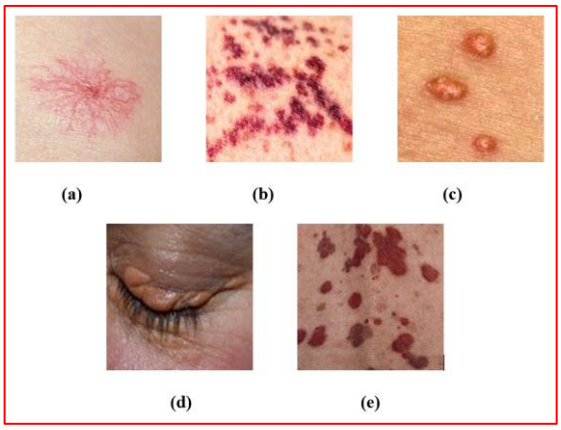

Fig. 9. Skin Manifestations of Liver

The Fig. 9 show the actual image of the 5 skin manifestations of liver that will be cover in this study. These are (a) Spider Angioma, (b) Purpura, (c) Eruptive Xanthoma, (d) Xanthelasma, and (e) Leukocytoclastic Vasculitis.

A. Data Acquisition and Collection

TABLE I. Total Number of Raw Datasets

Skin Manifestations of Liver	No. of Datasets
Spider Angioma	905
Purpura	1215
Eruptive Xanthoma	1011
Xanthelasma	1975
Leukocytoclastic Vasculitis	1085
Total	**6191**

The table 1 shows the total number of raw datasets per skin manifestation of liver. These are raw images from various dermatological websites.

TABLE II. Total Number of Trained Datasets in the Machine Learning

Skin Manifestations of Liver	Training Set	Testing Set	Validation Set
Spider Angioma	634	181	90
Purpura	851	243	121
Eruptive Xanthoma	708	202	101
Xanthelasma	1383	395	197
Leukocytoclastic Vasculitis	760	217	108

The table 2 shows the lists of the segmentation of datasets per training, testing, and validation. The Training set is composed of 70% of the total number of raw datasets while the testing datasets is 20% and the validation set is 10%.

TABLE III. Total Number of Annotated Merge Trained Datasets

Training Set	Validation Set	Testing	Total
6930	660	332	7922

The table 3 display the total count of augmented datasets generated through Roboflow, all of which were annotated for training purposes by the 7 CNN Models utilizing Google Colab.

B. Hardware Construction

The integration of the components of the prototype is displayed in this section. Also, the proposed designed model prototype of the camera. Python will be used to program the Raspberry Pi and to train and test the datasets through Machine Learning Algorithms. It is a high-level and widely used programming language for machine learning and image processing.

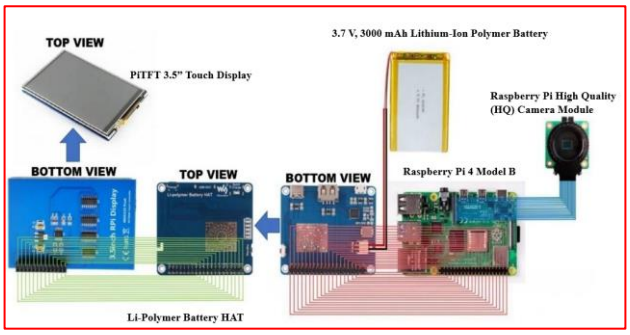

Fig. 10. Wiring of the Analytic Camera

The Fig 10 shows the wiring of the electronic components for the Analytic Camera. This will be as alternative for the Schematic Diagram due to unavailability of the Software Simulator for the components mentioned.

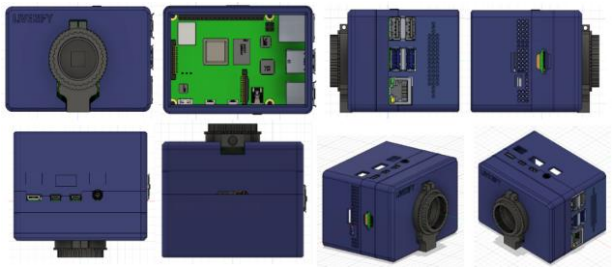

Fig. 11. Analytic Camera 3D Model

The Fig. 11 shows the representation of the prototype enclosure with the raspberry pi 4 model b and the camera module using the 360 Fusion.

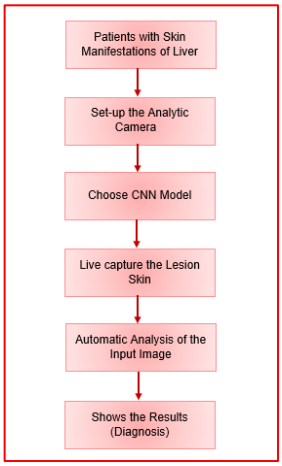

Fig. 12. Analytic Camera Test Process Flow Chart

The Fig. 12 shows the flowchart of the step-by-step process of how to use the analytic camera by a user. This will be the guide in the deployment process to detect liver diseases by lesion skin analysis. However, the results that will be shown are in the range which means that generated liver stage/s and liver disease/s is not accurately having all of it. The final diagnosis is still by a Physician (Hepatologist).

C. Mobile Application

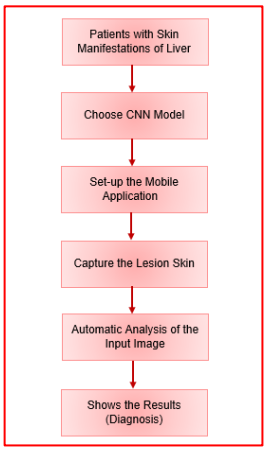

Fig. 13. Mobile Application Test Process Flow Chart

The Fig. 13 shows the flowchart of the step-by-step process of how to use the developed mobile application by a user. This will be the guide in the deployment process to detect liver diseases by lesion skin analysis. However, the results that will be shown are in the range which means that generated liver stage/s and liver disease/s is not accurately having all of it. The final diagnosis is still by a Physician (Hepatologist).

D. Utilization of machine learning algorithms specifically the 7 CNN Models (YOLO v5, DenseNet, MobileNet, VGG 16, Xception, ResNet-50, Inception - Resnet v2) in the program of the analytic camera and mobile applications for the 5 skin manifestations of liver diseases

In this study, there are seven Convolutional Neural Network (CNN) models will be established to utilize the feature extraction of the raw images. These models are DenseNet, MobileNet, VGG 16, YOLO v5, Xception, ResNet-50, and Inception - Resnet v2. Each model has advantages and disadvantages which will be analyzed to determine which model is best suited for this study.

E. Comparison of the analytic camera to a mobile camera (applications) in performing the accuracy of lesion skin analysis with the different CNN models

In this study, the analytic camera and the mobile application will be compared to test the accuracy of the lesion skin analysis results based on the stand-alone hardware and software development abilities. The skin lesion image will be captured by the analytic camera and the mobile phone, and it will be processed to examine for any potential liver diseases with the application of the 7 CNN Models.

F. Determination of which CNN model is the best for the detection of the five skin manifestations of the liver through Validation Tests

A Convolutional neural network (CNN) is a neural network that has one or more convolutional layers and is used mainly for image processing, classification, segmentation, and for other auto-correlated data. It is also the most recent machine-learning algorithm for liver diseases in medical imaging. The process includes the extraction of imaging features, convolved operation, normalization, and rectified linear units (ReLU) operation. There are seven selected models (YOLO v5, DenseNet, MobileNet, VGG 16, Xception, ResNet-50, Inception - Resnet v2) of CNN that will be applied to the study to determine which of these models is best suited for this kind of study.

G. Testing and validation of the effectiveness of the device and application through deployment in a selected hospital or clinic

This study requires testing and validation of the effectiveness of the device and application through deployment in the selected hospitals. The device and application are used to detect skin diseases (Spider Angioma, Purpura, Eruptive Xanthoma, Xanthelasma, and

Leukocytoclastic Vasculitis) to determine liver disease/s and its progression. During the deployment process, the gathering of data is done by testing 10-15 patients having the mentioned skin manifestations. It is a non-invasive method; therefore, it will not harm or cause any risk to the human subject upon testing because the process is through skin image capturing using the Analytic camera and the mobile applications that are programmed for liver disease detection through lesion skin analysis only. However, the results that will be shown are in the range which means that generated liver stage/s and liver disease/s is not accurately having all of it. The final diagnosis is still by a Physician (Hepatologist).

IV. RESULTS AND DISCUSSION

A. Analytic Camera

The Analytic Camera is an integrated Raspberry Pi camera that can analyze lesion skin of the 5 skin manifestations of the liver. The Machine Learning Algorithms of the program are embedded with 7 CNN models that can be used for detection.

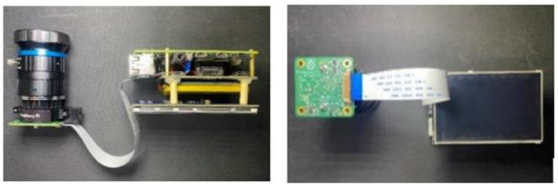

(a) (b)

Fig. 1. Integration of Components

The Fig. 1 shows (a) the integration of Raspberry Pi 4 Model B and the Raspberry Pi High Quality (HQ) Camera with 16mm Camera Lens (C-Mount). (b) shows the connection of the microprocessor with the PiTFT 3.5" Touch Display and the camera module,

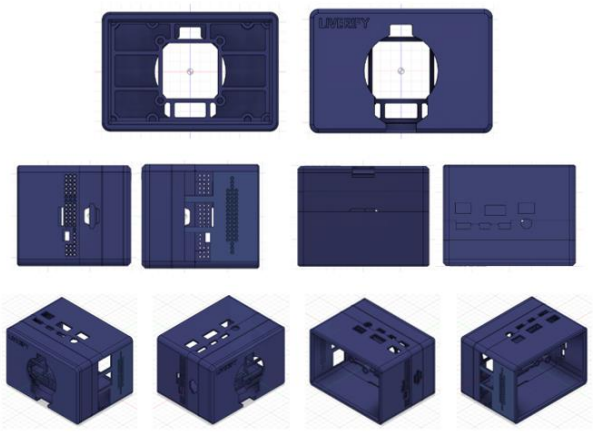

Fig. 2. 3D Case Layout

The Fig. 2 displays the physical layout of the Analytic Camera, providing a comprehensive 3D view with a 360-degree perspective.

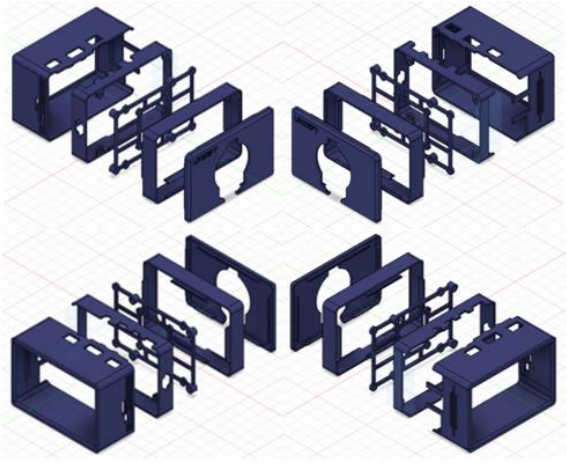

Fig. 3. 3D Case Layers

The Fig. 3 illustrate the detailed layering of each component within the prototype's enclosure, providing a comprehensive view of the enclosure's construction.

Fig. 4. Analytic Camera Construction

The Fig. 4 shows the actual Analytic camera after the integration of the components and the case.

TABLE I. Analytic Camera Validation Test Results

CNN Models	Analytic Camera	
	Correctly Detected	Detection Failed
YOLO v5	30	0
DenseNet	1	29
Mobilenet	9	21
VGG 16	20	10
Xception	21	9
ResNet-50	8	22
Inception-Resnet v2	14	16

The table 1 provides the results of validation tests conducted on the analytic camera. The tests were performed on a validation dataset that was not part of the datasets used to train the 7 CNN models applied to the program of the device and application. YOLO v5 achieved a perfect score of 30 out of 30, indicating 100% accuracy. However, the other CNN models performed less effectively. Xception detected 21 out of 30, VGG 16 detected 20 out of 30, Inception-ResNet v2 detected 14 out of 30, Mobilenet detected 9 out of 30, ResNet-50 detected 8 out of 30, and DenseNet detected only 1 out of 30.

B. Mobile Applications

The Mobile Application is a CNN model-based application that can analyze lesion skin of the 5 skin manifestations of the liver. There are 7 developed

applications for different embedded Machine Learning Algorithms in the program that can be used for detection.

Fig. 5. Liverify App

The Fig. 5 shows the graphical user interface of the developed mobile application. It is a one-touch process of capturing the lesion skin and it will automatically display the results.

TABLE II. Liverify Application Validation Test Results

CNN Models	Liverify App	
	Correctly Detected	Detection Failed
YOLO v5	22	8
DenseNet	17	13
Mobilenet	20	10
VGG 16	19	11
Xception	20	10
ResNet-50	18	12
Inception-Resnet v2	20	10

The table 2 provides the results of validation tests conducted on the Liverify App using a validation dataset that was not part of the datasets used to train the 7 CNN models applied to the program of the device and application. YOLO v5 achieved the highest detection rate with 22 out of 30. However, the other CNN models performed less effectively. MobileNet, Xception, and Inception-ResNet v2 detected 20 out of 30, while ResNet-50 detected 18 out of 30, VGG 16 detected 19 out of 30, and DenseNet detected only 17 out of 30.

C. Machine Learning Algorithms (CNN Models)

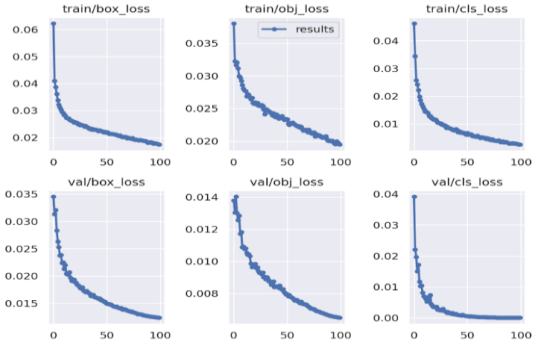

Fig. 6. Training Loss Indicators using YOLO v5

The YOLOv5 model effectively detects and predicts six specific classes during training. The graph illustrates the accuracy percentages against the number of training epochs (100 epochs). Lower values of box_loss, objectness_loss, and classification_loss indicate better object prediction performance. Both the training and validation results demonstrate accurate detection and classification of the classes. The graph depicts the changes in box_loss and object_loss over the epochs, reflecting variations in these losses over time. Box_loss represents the model's precision in determining object centers and bounding boxes, while object_loss relates to the likelihood of objects not existing within proposed regions and is inversely related to objectness. Classification_loss measures the model's accuracy in predicting object classes. The model shows excellent precision and positional mean. Furthermore, the box_loss, object_loss, and classification_loss for the validation data show significant improvement. Our findings indicate low error percentages in training the datasets, with box_loss and objectness_loss at 1% each, and classification_loss at 0%. These low error percentages signify successful training outcomes for our datasets.

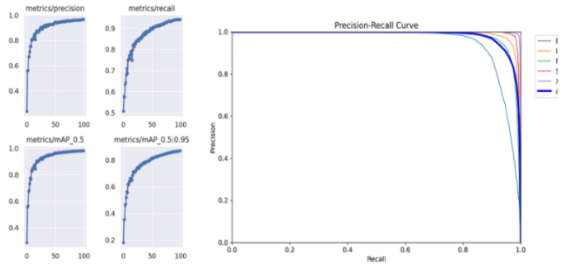

Fig.7. Precision-Recall Results of the Trained Datasets Using YOLO v5

Fig. 7 displays the Precision and Recall measures, where Precision assesses bbox prediction accuracy, and Recall measures the percentage of correctly predicted true bboxes. Our results show a Precision of 100% and a nearly 100% Recall, indicating high accuracy. The Precision-Recall curve is a valuable tool for evaluating the object detector's performance by adjusting the confidence level threshold. A higher confidence value indicates greater certainty in object detection. Analyzing the curve helps us understand how the model's performance changes with varying confidence thresholds. The term "mAP_0.5" refers to the mean Average Precision (mAP) at an IoU threshold of 0.5. Remarkably, the Precision-Recall curve for the YOLOv5 model shows all five classes achieving a mAP of 100%, demonstrating outstanding performance.

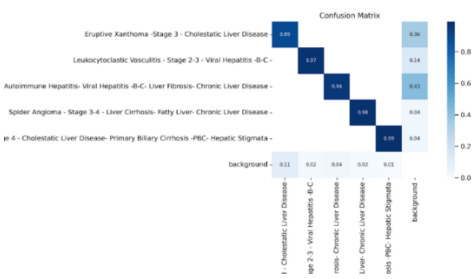

Fig. 8. Detection Accuracy Results of the Trained Datasets Using YOLO v5

The Fig. 8 shows the confusion matrix of the Yolov5 to our datasets. Also, the detection of each class is successful.

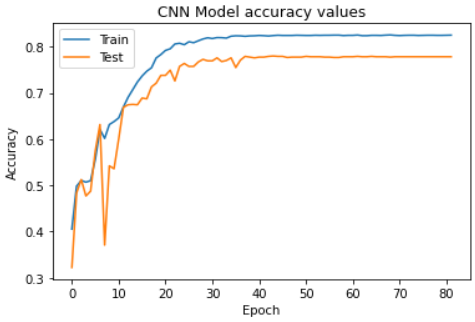

Fig. 9. Accuracy Results of the Trained Datasets Using DenseNet

The Fig. 9 shows the accuracy values of the training model DenseNet. The highest accuracy value attained was at 82.49% while the lowest was at 40.53%.

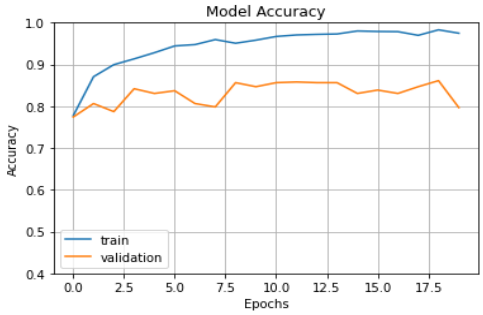

Fig. 10. Accuracy Results of the Trained Datasets Using Mobilenet

The Fig. 10 shows the accuracy values of the training model Mobilenet. The highest accuracy value attained was at 98.29% while the lowest was at 78%.

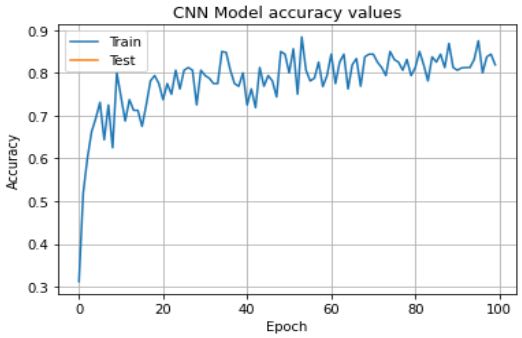

Fig. 11. Accuracy Results of the Trained Datasets Using VGG 16

The Fig. 11 shows the accuracy values of the training model VGG 16. The highest accuracy value attained was at 88.41% while the lowest was at 32%.

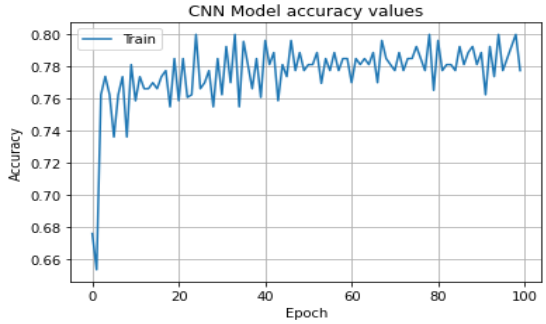

Fig. 12. Accuracy Results of the Trained Datasets Using Xception

The Fig. 12 shows the accuracy values of the training model Xception. The highest accuracy value attained was at 80% while the lowest was at 65.38%

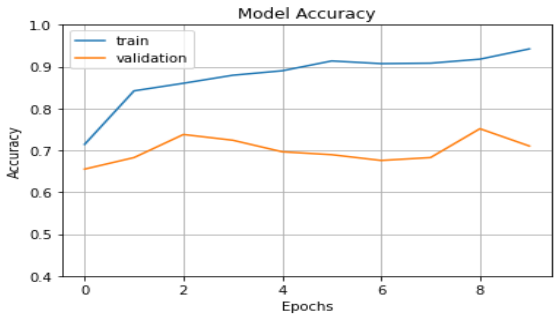

Fig. 13. Accuracy Results of the Trained Datasets Using ResNet-50

The Fig. 13 shows the accuracy values of the training model ResNet50. The highest accuracy value attained was at 92% while the lowest was at 68%.

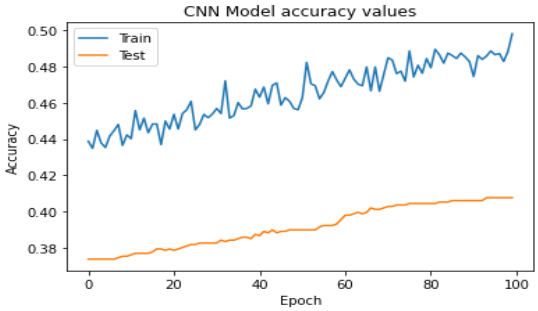

Fig. 14. Accuracy Results of the Trained Datasets Using Inception-Resnet v2

The Fig. 14 shows the accuracy values of the training model Inception-Resnet v2. The highest accuracy value attained was at 49.79% while the lowest was at 43.88%.

D. Comparison of Mobile Application and Analytic Camera

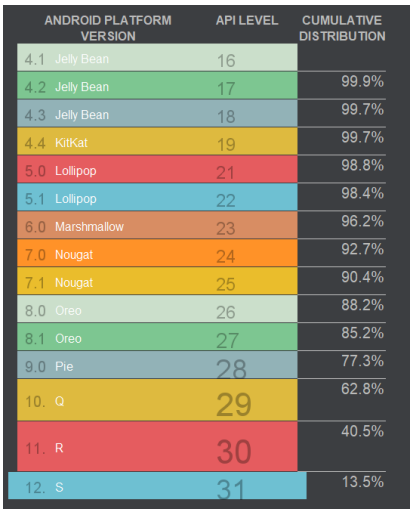

Figure 15. Mobile Camera Set Requirement

The Fig. 15 shows the indicated set requirement of the mobile phone for the developed application to analyze the lesion skin accurately and detect the possible liver diseases linked to the skin manifestation/s.

TABLE III. Validation Tests Summary

CNN Models	Analytic Camera		Total	Mobile Application		Total
	Detected	Failed		Detected	Failed	
YOLO v5	30	0	30	22	8	30
DenseNet	1	29	30	17	13	30
Mobilenet	9	21	30	20	10	30
VGG-16	20	10	30	19	11	30
Xception	21	9	30	20	10	30
ResNet-50	8	22	30	18	12	30
Inception - Resnet	14	16	30	20	10	30
Total	103	107	210	136	74	210

The table 3 displays the results of 210 validation tests carried out on both the Analytic Camera and the Mobile Application. In each test, a CNN model was used to examine 5 skin manifestations of the liver, with 6 samples for each manifestation. The Analytic Camera detected 103 instances out of the 210 tests, while the Mobile Application detected 136 instances. However, this data is for the purpose of the comparison of the Machine Learning algorithms in terms of accuracy detection of the device and mobile camera (application) through lesion skin analysis.

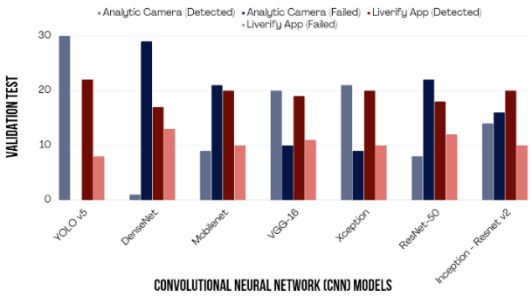

Fig. 16 Validation Test Results of the Analytic Camera and Mobile Camera (Liverify App)

The Fig. 16 presents the outcomes of 30 validation tests carried out on both the Analytic Camera and the Mobile Application, utilizing seven Convolutional Neural Network models. Each set of tests comprised 5 skin manifestations of the liver with 6 samples each. Based on the results, the CNN model YOLO v5 was able to correctly analyze 30 lesion skins using the Analytic Camera. Following that, Xception had 21, VGG 16 had 20, Inception-ResNet v2 had 14, Mobilenet had 9, ResNet-50 had 8, and DenseNet had 1. In contrast, for the Mobile Application, the YOLO v5 model was able to correctly analyze 22 lesion skins. However, Xception, Inception-ResNet v2, and Mobilenet all had 20 correct analyses, while VGG 16 had 19, ResNet-50 had 18, and DenseNet had 17.

E. Convolutional Neural Network (CNN) Model Analysis

TABLE IV. CNN Model Analysis

CNN Models	Analytic Camera		Liverify App	
	Detection Model Results	Model Accuracy	Detection Model Results	Model Accuracy
YOLO v5	1	100%	0.7333333333	73.33%
DenseNet	0.03333333333	3.33%	0.5666666667	56.67%
Mobilenet	0.3	30%	0.666666667	66.67%
VGG 16	0.6666666667	66.67%	0.6333333333	63.33%
Xception	0.7	70%	0.666666667	66.67%
ResNet-50	0.2666666667	26.67%	0.6	60%
Inception-ResNet v2	0.4666666667	46.67%	0.666666667	66.67%

The table 4 presents the validation results for the accuracy of lesion skin analysis detection by seven Convolutional Neural Network (CNN) models on skin manifestations of the liver. Through validation tests, it predicts that the best CNN model based on the 210 validation tests results with the highest accuracy. Based on the detection percentage, the best CNN model for the Analytic Camera is YOLO v5 with a value of 1, followed by Xception with a value of 0.7, VGG 16 with 0.6667, Inception-ResNet v2 with 0.4667, Mobilenet with 0.3, ResNet-50 with 0.2667, and DenseNet with 0.0333. Similarly, for the Mobile Application, the detection model results for YOLO v5 is 0.7333. However, Xception, Inception-ResNet v2, and Mobilenet have a value of 0.6667, VGG 16 has 0.6333, ResNet-50 has 0.6, and DenseNet has 0.5667.

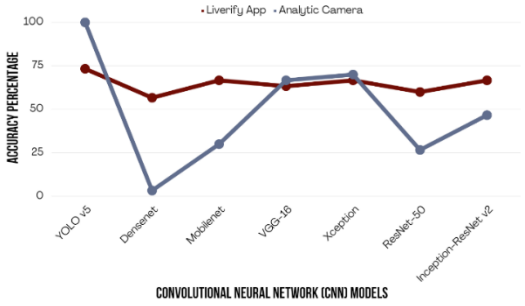

Fig. 17. CNN Model Percentage Accuracy

The Fig. 17 depicts the accuracy percentages of seven Convolutional Neural Network (CNN) models in detecting lesion skin analysis using the analytic camera. YOLO v5 has the highest accuracy percentage of 100%, followed by Xception with 70%, VGG 16 with 66.67%, Inception-ResNet v2 with 46.67%, Mobilenet with 30%, ResNet-50 with 26.67%, and DenseNet with 3.33%. Similarly, in the case of the mobile application, YOLO v5 has the highest accuracy percentage of 73.33%. Xception, Inception-ResNet v2, and Mobilenet have the same accuracy percentage of 66.67%, while VGG 16 has 63.33%, ResNet-50 has 60%, and DenseNet has 56.67%.

F. Validation

TABLE V. Benchmarking Accuracy Evaluation

Skin Disease	Analytic Camera		Liverify App	Gastroenterologist's Diagnosis		Analysis
	Liver Diseases	Liver Stages		Tests Conducted	Liver Diseases	
Spider Angioma	Liver Cirrhosis Fatty Liver Disease	Stage 3: Fibrosis Stage 4: Cirrhosis	Spider Angioma is detected as Purpura on the 1st test and Leuko-cytoclastic Vasculitis on the 2nd test	Health History Physical Examination Ultrasound (UTZ) Magnetic Resonance Imaging (MRI) Computerized Tomography (CT) Scan	Liver Cirrhosis (Cirrhosis 2: Alcohol Liver Disease) Fatty Liver Disease *Note: The patient is also diagnosed with Type 2 Diabetes Mellitus (T2DM).*	True Positive

The table 5 shows the benchmarking accuracy evaluation between the analytic camera and the mobile application using the best CNN model, YOLO v5. The device detected the skin disease of the patient on the first trial as Spider Angioma. The camera has a 16mm lens that was able to microscopically analyze the lesion skin.

However, the mobile application encountered difficulty in detection as the Spider Angioma is so tiny that it cannot focus the camera itself to clearly capture every detail of the skin disease and detect it accurately. On the first trial, it detected the Spider Angioma as Purpura while on the 2nd trial as Leukocytoclastic Vasculitis.

A resident Gastroenterologist in Justice Jose Abad Santos General Hospital diagnosed the 67 years old male patient with Liver Cirrhosis specifically Cirrhosis 2: Alcohol Liver Disease and Fatty Liver Disease. These liver diseases were found through healthy history checks, physical examination, ultrasound, Magnetic Resonance Imaging (MRI), and Computerized Tomography (CT) Scan. The diagnoses are similar to the Analytic Camera's results which are through the non-invasive method of lesion skin capturing and analyzing the image through a Machine Learning Algorithm embedded into the device. Therefore, it is true positive. However, the other CNN Models were also tested but all had difficulty in detection.

G. Summary and Findings

The automated liver detection using Analytic Camera and Mobile Camera (application) were tested in performing the accuracy of lesion skin analysis of the 5 skin manifestations of the liver (Spider Angioma, Purpura, Eruptive Xanthoma, Xanthelasma, and Leukocytoclastic Vasculitis) with the 7 Convolutional Neural Network (CNN) models evaluated through validation tests analysis and deployment.

The different Machine Learning Algorithms were trained and tested before embedding into the program. The YOLO v5 displays the train and validation test reached to the 0.06 to 0.015 onwards in 0 to 100 epochs which means that the datasets are trained successfully. On the other hand, DenseNet has training model accuracy of 40.53% to 82.49%, Mobilenet is 78% to 98.29%, VGG 16 is 32% to 88.41%, Xception is 65.38% to 80%, ResNet50 is 68% to 92%, and Inception-Resnet v2 is 43.88% to 49.79% training model accuracy.

Validation test analysis can help predict the best CNN model with the highest accuracy for lesion skin analysis detection. The YOLO v5 CNN model is determined to be the best with equivalent detection accuracy of 100% when using the Analytic Camera with 210 validation tests. The Xception model follows with 70% accuracy, while VGG 16 has 66.67% accuracy, Inception-ResNet v2 has 46.67% accuracy, Mobilenet has 30% accuracy, ResNet-50 has 26.67% accuracy, and DenseNet has 3.33% accuracy. For Mobile Applications, the YOLO v5 model has 73.33% accuracy, followed by Xception, Inception-ResNet v2, and Mobilenet with 66.67% accuracy, VGG 16 with 63.33% accuracy, ResNet-50 with 60% accuracy, and DenseNet with 56.67% accuracy in lesion skin analysis detection.

The analytic camera, the mobile application utilizing YOLO v5, and the physician's diagnosis were compared for benchmarking accuracy. The analytic camera successfully identified the skin disease on the first attempt as Spider Angioma due to its 16mm lens, which allowed for microscopic analysis of the lesion skin. However, the mobile application had difficulty detecting Spider Angioma, initially identifying it as Purpura and later as Leukocytoclastic Vasculitis on the second attempt. The patient was diagnosed with Liver Cirrhosis, specifically Cirrhosis 2: Alcohol Liver Disease and Fatty Liver Disease, by a resident Gastroenterologist in Justice Jose Abad Santos General Hospital through traditional methods such as history checks, physical examination, ultrasound, Magnetic Resonance Imaging (MRI), and Computerized Tomography (CT) Scan. The analytic camera's non-invasive method of lesion skin capturing and analysis through a machine learning algorithm embedded in the device yielded similar results to the physician's diagnosis. However, all other CNN models tested encountered difficulty in detection.

V. CONCLUSION

The following conclusion has been made based on the results and findings obtained:

The analytic camera was successfully constructed by integrating a Raspberry Pi 4 Model B with a 16mm camera lens for the purpose of detecting skin lesions through the embedding of machine learning algorithms. Similarly, the development of mobile applications was also successful as different CNN models were executed separately using a common graphical user interface (GUI).

The program for the analytic camera and mobile applications successfully utilized seven CNN models, namely YOLO v5, DenseNet, MobileNet, VGG 16, Xception, ResNet-50, and Inception - Resnet v2, to detect five skin manifestations of liver diseases and test their accuracy. Among the models, YOLO v5 showed higher accuracy with training and validation tests reaching 0.06 to 0.015 in 0 to 100 epochs, indicating successful training of the datasets. This model also demonstrated better training dataset accuracy compared to the other CNN models.

The mobile camera (application) showed 64.76% accuracy in detecting skin lesions among all 7 CNN models, with a detection rate of 136 out of 210 skin diseases. However, the device with the YOLO v5 CNN model displayed 100% accuracy in lesion skin analysis. It appears that YOLO v5 performed significantly better than the other CNN models in detecting skin manifestations of the liver using the analytic camera.

Based on the results of 210 validation test analysis, the YOLO v5 CNN model was found to be the most effective in detecting the five skin manifestations of liver disease. The decision analysis revealed that the Analytic Camera with the YOLO v5 model achieved a result of 1, indicating a model accuracy of 100%. The mobile camera application achieved a detection value of 0.7333, which is equivalent to a model accuracy of 73.33%.

The functionality of the device and mobile applications were evaluated based on the liver patient test and survey with the Gastroenterologist at Justice Jose Abad Santos General Hospital, Internal Medicine Department. The evaluation showed that the analytic camera using YOLO v5 CNN model has moderate accuracy, as demonstrated by the test conducted on a liver patient and the analysis of the device's capabilities by the gastroenterologist. This is because only one patient was tested in the actual setup, and the occurrence of skin manifestations of the liver is rare, with an approximate incidence of 33%, and liver damage ranges from 50% to 75%.

VI. RECOMMENDATIONS

To further improve the study, the researchers recommend the following:

To ensure optimal performance of the Analytic Camera, the researchers propose using a high-speed microcontroller to prevent device lag. In addition to real-time capture, it is suggested to include a capture mode in the graphical user interface (GUI) and a full-screen mode to enhance the functionality of the Analytic Camera. Furthermore, improving the physical structure of the camera is advised to enable convenient testing of patients, such as incorporating a minimum 7" LCD touchscreen for easy configuration, a stable camera position setup, and a camera lens light to mitigate the impact of lighting conditions on capturing skin lesions, which can affect the accuracy of the analysis.

In the Machine Learning Algorithm, updating the latest Convolutional Neural Network (CNN) Model to improve the quality of detection based on the newest and latest trend. Thousands of datasets which include variations of skin color and elasticity are highly recommended to improve the level of intelligence of the program in detection.

To facilitate a more effective comparison between the analytic camera and the mobile app, the researchers suggest utilizing a camera lens that can be easily attached to the phones' built-in cameras.

To have a higher accuracy of liver disease detection, the researchers recommend adding more parameters of skin manifestations (e.g., Jaundice, Palmar Erythema, Telangiectasia) that a liver patient commonly has than the skin diseases covered in this study which are very rare.

Include the health history background (history of Hepatitis or Diabetes that makes a patient at risk for Non-Alcoholic Fatty Liver Disease) and physical examination in the program as the first step to do before conducting the non-invasive test for the lesion skin analysis which will be one of the factors for the percentage accuracy test of the Analytic Camera to diagnosed liver diseases other than the skin manifestations as this is one of the factors that a Physician do before other invasive tests conducted.

REFERENCES

[1] "Skin diseases: Types of, symptoms, treatment & prevention," Cleveland Clinic. [Online]. Available: https://my.clevelandclinic.org/health/diseases/21573-skin-diseases

[2] A. Bhandari and R. Mahajan, "'Skin Changes in Cirrhosis,'" J. Clin. Exp. Hepatol., vol. xxx, no.xxx, 2022, doi: 10.1016/j.jceh.2021.12.013.

[3] B. Wedro and B. Anand, "Liver Disease," MedicineNet. [Online]. Available: https://www.medicinenet.com/liver_disease/article.htm

[4] "Liver disease," Mayo Clinic. [Online] Available: https://www.mayoclinic.org/diseasesconditions/liver-problems/symptoms-causes/syc-20374502

[5] "Liver Disease in Philippines" World Life Expectancy. [Online]. Available: https://www.worldlifeexpectancy.com/philippines-liver-disease

[6] "Non communicable diseases," World Health Organization. [Online]. Available: https://www.who.int/news-room/fact-sheets/detail/noncommunicable-diseases

[7] A. Koulaouzidis, S. Bhat, and J. Moschos, "Skin manifestations of liver diseases," Ann. Hepatol., vol. 6, no. 3, pp. 181–184, 2007, doi: 10.1016/s1665-2681(19)31926-x.

[8] "The Progression of Liver Disease," American Liver Foundation. [Online]. Available: https://liverfoundation.org/for-patients/about-the-liver/the-progression-of-liver-disease/#cirrhosis-severe-scarring

[9] H. Rifai, "Liver Disease Detection from CT scan images using Deep Learning and Transfer Learning," 2020.

[10] D. H. Belavigi, G. S. Veena, and D. Harekal, "Prediction of liver disease using Rprop, SAG and CNN," Int. J. Innov. Technol. Explor. Eng., vol. 8, no. 8, pp. 3290–3295, 2019.

[11] B. Sathelly, "An Artificial Neural Network Approach to Predict Liver Failure Likelihood." 2018. [Online]. Available: http://rave.ohiolink.edu/etdc/view?acc_num=toledo1535112414430542

[12] I. U. R. Rahim et al., "Skin, mucosal, nail and hair manifestations in 100 patients of chronic liver disease (CLD)," Pakistan J. Med. Heal. Sci., vol. 12, no. 2, pp. 602–604, 2018.

[13] A. D. Patel, K. Katz, and K. B. Gordon, "Cutaneous manifestations of chronic liver disease," Clinics in Liver Disease, vol. 24, no. 3, pp. 351–360, Aug. 2020.

[14] M. Ralli, F. Candelori, A. Di Stadio, and M. de Vincentiis, "Spider Angioma of the Nasal Mucosa," Ear, Nose Throat J., pp. 1–2, 2020, doi: 10.1177/0145561320980202.

[15] B. Karnath, "Stigmata of Chronic Liver Disease," in Definitions, no. July, Qeios, 2020, pp. 14–17. doi: 10.32388/VLAYG1.

[16] D. M. Aloise and G. Izquierdo, "Uncertainty of Liver Cirrhosis Diagnosis and Use of Elastography," Cureus, vol. 13, no. 9, Sep. 2021, doi: 10.7759/cureus.18411.

[17] S. Ohtaki et al., "Eruptive xanthomas as a marker for metabolic disorders: A specific form of xanthoma that reflects hypertriglyceridemia," Clin. Case Reports, vol. 10, no. 4, 2022, doi: 10.1002/ccr3.5671.

[18] T. A. Nessel, C. C. Kerndt, J. A. Bills, and L. Sikorski, "Eruptive xanthomas: a warning sign of future hyperlipidemia complications," Int. J. Res. Dermatology, vol. 6, no. 4, p. 579, 2020, doi: 10.18203/issn.2455-4529.intjresdermatol20202672.

[19] S. Y. Lee and C. A. Sheth, "Eruptive xanthoma associated with severe hypertriglyceridemia and poorly controlled type 1 diabetes mellitus," J. Community Hosp. Intern. Med. Perspect., vol. 9, no. 4, pp. 344–346, 2019, doi: 10.1080/20009666.2019.1650591.

[20] H. Wade et al., "Eruptive xanthomas secondary to severe hypertriglyceridemia," Glob. J. Med. Clin. Case Reports, vol. 8, pp. 112–115, Oct. 2021, doi: 10.17352/2455-5282.000142.

[21] M. Kashif, H. Kumar, and M. Khaja, "An unusual presentation of eruptive xanthoma: A case report and literature review," Med. (United States), vol. 95, no. 37, pp. 10–12, 2016, doi: 10.1097/MD.0000000000004866.

[22] P.A. Nair, C.R. Patel, J.D. Ganjiwale, N.G. Diwan, N.B. Jivani. "Xanthelasma palpebrarum with arcus cornea: A clinical and biochemical study". Indian J Dermatol, vol 61, no. 3, pp. 295-300, 2016

[23] H. W. Chen, J. C. Lin, Y. H. Wu, and Y. L. Chiu, "Risk of non-alcoholic fatty liver disease in xanthelasma palpebrarum," J. Inflamm. Res., vol. 14, pp. 1891–1899, 2021, doi: 10.2147/JIR.S305694.

[24] Y. H. Chung, S. Y. Kang, and W. S. Choi, "A case of intramuscular xanthelasma palpebrarum found during blepharoplasty," Arch. Craniofacial Surg., vol. 19, no. 4, pp. 296–299, 2018, doi: 10.7181/acfs.2018.02068.

[25] G. de Ferreira, A. L. Watanabe, N. de Trevizoli, F. M. Jorge, L. G. Diaz, M. C. Araujo, G. de Araujo, and A. de Machado, "Leukocytoclastic vasculitis caused by hepatitis C virus in a liver transplant recipient: A case report," World Journal of Hepatology, vol. 11, no. 4, pp. 402–408, 2019.

[26] S. Sandhu et al., "Leukocytoclastic vasculitis as a cutaneous manifestation of ChAdOx1 nCoV-19 corona virus vaccine (recombinant)," Dermatol. Ther., vol. 34, no. 6, pp. 1–4, 2021, doi: 10.1111/dth.15141.

[27] G. Fiorillo et al., "Leukocytoclastic vasculitis (cutaneous small-vessel vasculitis) after COVID-19 vaccination," J. Autoimmun., vol. 127, no. December 2021, p. 102783, 2022, doi: 10.1016/j.jaut.2021.102783.

[28] M. A. Reyes and L. F. Eichenfield, “Purpura,” Princ. Pract. Pediatr. Infect. Dis., pp. 451-455.e1, Jan. 2018, doi: 10.1016/B978-0-323-40181-4.00071-2.
[29] S. Mohammad, B. Chandio, A. A. Soomro, S. Lakho, Z. Ali, and F. Shaukat, “The Frequency of Cutaneous Manifestations in Hepatitis C: A Cross-sectional Study in a Tertiary Care Hospital in Pakistan,” Cureus, vol. 11, no. 11, pp. 9–12, 2019, doi: 10.7759/cureus.6109.
[30] L. Kuna, J. Jakab, R. Smolic, G. Y. Wu, and M. Smolic, “HCV extrahepatic manifestations,” J. Clin. Transl. Hepatol., vol. 7, no. 2, pp. 172–182, 2019, doi: 10.14218/JCTH.2018.00049.
[31] B. Fernandes et al., “Rheumatologic manifestations of hepatic diseases,” Ann. Gastroenterol., vol. 32, no. 4, pp. 352–360, 2019, doi: 10.20524/aog.2019.0386.
[32] L. Safira, B. Irawan, and C. Setiningsih, “Implementation of the Certainty Factor Method for Early Detection of Cirrhosis Based on Android,” J. Phys. Conf. Ser., vol. 1201, no. 1, 2019, doi: 10.1088/1742-6596/1201/1/012053.
[33] B. Sathelly, “An Artificial Neural Network Approach to Predict Liver Failure Likelihood.” 2018. Accessed: Jun. 06, 2022. [Online]. Available: http://rave.ohiolink.edu/etdc/view?acc_num=toledo1535112414430542
[34] K. V. Swamy and B. Divya, "Skin Disease Classification using Machine Learning Algorithms," 2021 2nd International Conference on Communication, Computing and Industry 4.0 (C2I4), 2021, pp. 1-5, doi: 10.1109/C2I454156.2021.9689338.
[35] J. Gao, Q. Jiang, B. Zhou, and D. Chen, “Convolutional neural networks for computer-aided detection or diagnosis in medical image analysis: An overview,” Math. Biosci. Eng., vol. 16, no. 6, pp. 6536–6561, 2019, doi: 10.3934/mbe.2019326.
[36] M. Koenigkam Santos, J. Raniery Ferreira Júnior, D. Tadao Wada, A. Priscilla Magalhães Tenório, M. Henrique Nogueira Barbosa, and P. Mazzoncini De Azevedo Marques, “Artificial intelligence, machine learning, computer-aided diagnosis, and radiomics: Advances in imaging towards to precision medicine,” Radiol. Bras., vol. 52, no. 6, pp. 387–396, 2019, doi: 10.1590/0100-3984.2019.0049.
[37] H. Moghassemi, R. Rabiei, H. Moghaddasi, M. Shabani, and R. Ataee, “Computer-Aided Diagnosis Approaches to Fatty Liver Disease According to Sonographic Images Based on Wavelet Transform: A Review Study,” J. Clin. Rev. Case Reports, vol. 3, no. 4, 2018, doi: 10.33140/jcrc/03/04/00007.
[38] P. R. Kshirsagar, H. Manoharan, S. Shitharth, A. M. Alshareef, N. Albishry, and P. K. Balachandran, “Deep Learning Approaches for Prognosis of Automated Skin Disease,” Life, vol. 12, no. 3, p. 426, 2022, doi: 10.3390/life12030426.
[39] A. A. Elngar, R. Kumar, A. Hayat, and P. Churi, “Intelligent System for Skin Disease Prediction using Machine Learning,” J. Phys. Conf. Ser., vol. 1998, no. 1, 2021, doi: 10.1088/1742-6596/1998/1/012037.
[40] J. Velasco et al., “A smartphone-based skin disease classification using mobilenet CNN,” Int. J. Adv. Trends Comput. Sci. Eng., vol. 8, no. 5, pp. 2632–2637, 2019, doi: 10.30534/ijatcse/2019/116852019.
[41] N. S. Alkolifi Alenezi, “A Method of Skin Disease Detection Using Image Processing and Machine Learning,” Procedia Comput. Sci., vol. 163, pp. 85–92, 2019, doi: 10.1016/j.procs.2019.12.090.
[42] R. van de Schoot et al., “Bayesian statistics and modelling,” Nature Reviews Methods Primers, vol. 1, no. 1, pp. 1–26, Jan. 2021, doi: 10.1038/s43586-020-00001-2.
[43] “Bayesian Statistics: A Beginner’s Guide | QuantStart,” www.quantstart.com. https://www.quantstart.com/articles/Bayesian-Statistics-A-Beginners-Guide/